Glasslike Two-Level Systems in Minimally Disordered Mixed Crystals

J. P. Wrubel, B. E. Hubbard, N. I. Agladze, and A. J. Sievers
Laboratory of Atomic and Solid State Physics, Cornell University, Ithaca, New York 14853-2501, USA

P. P. Fedorov
Institute of General Physics, 117942 Moscow, Russia

D. I. Klimenchenko and A. I. Ryskin
S. I. Vavilov State Optical Institute, 199034 St. Petersburg, Russia

J. A. Campbell
Department of Physics, University of Canterbury, Christchurch, New Zealand
(Received 18 November 2005; revised manuscript received 30 January 2006; published 16 June 2006)

THz spectroscopy is used to identify a broad distribution of two-level systems, characteristic of glasses, in the substitutional monatomic mixed crystal systems, $Ba_{1-x}Ca_xF_2$ and $Pb_{1-x}Ca_xF_2$. In these minimally disordered systems, two-level behavior, which was not previously known to occur, begins at a specific CaF_2 concentration. The concentration dependence, successfully modeled using the statistics of the impurity distribution in the lattice, points to a collective dopant tunneling mechanism.

DOI: 10.1103/PhysRevLett.96.235503 PACS numbers: 63.50.+x, 61.43.Fs, 78.30.Ly

The low temperature thermal properties of glasses and certain mixed crystals are dominated by a low lying distribution of excitations usually described within the phenomenological tunneling model as two-level systems (TLS) [1]. Although this TLS model is used to interpret the physics of disordered systems; justifications for either its assumptions or the well-known quantitative universality of fundamental physical characteristics have not been identified [2,3]. A related soft-potential model may have a greater range of applicability [4,5], but remains completely phenomenological. Other microscopic models which emphasize the potential energy landscape [6] have not yet provided new insights into the low temperature anomalies. After the discovery of TLS in chemically disordered mixed crystals [7,8] it became apparent that progressively disordered crystals, in which, unlike glasses, the saturation of TLS behavior had not been reached, offered good opportunities for exploring the fundamental mechanisms responsible for the broad distribution of low energy states [1]. So far TLS behavior in crystals has been demonstrated only in systems for which disorder is produced either by a low symmetry component with orientational degrees of freedom, or by chemical disorder. Extensive work on fluorite mixed crystals shows broad TLS-like behavior for aliovalent dopants in the range of 1–45 mol% [1,9]. There the substitutional dopant cation introduces charge compensating interstitial anions and clustering while at the same time producing local strain and electric fields due to the different components. In contrast, no TLS were observed in the isovalent mixed crystals $Ba_{1-x}Sr_xF_2$ [10].

In this Letter we report on a THz study of the low temperature properties of two isovalent mixed crystal series where glasslike TLS have been observed. Both $Ba_{1-x}Ca_xF_2$ and $Pb_{1-x}Ca_xF_2$ have the fluorite structure and with some difficulty, single crystals of high quality can still be produced, but only for $x \leq 0.1$. The appearance of TLS is consistent with the ideas that (1) the local dopant concentration varies statistically and (2) a critical concentration is required. The existence of glasslike TLS in these simple mixed crystals suggests that a very general tunneling mechanism is relevant.

Because of the decomposition of both $Ba_{1-x}Ca_xF_2$ and $Pb_{1-x}Ca_xF_2$ solid solutions under cooling, a high cooling rate is used during crystal growth. Solid solutions $Ba_{1-x}Ca_xF_2$ ($x = 0.02$, 0.04, 0.06, 0.08), crystal diameter 22 mm, crystal length 30 mm and $Pb_{1-x}Ca_xF_2$ ($x = 0.02$, 0.04, 0.06, 0.08, 0.10), crystal diameter 10 mm, crystal length 30 mm were grown by the Stockbarger-Bridgeman technique. The melt was maintained for 1.5 h at $T = 1400\,^{\circ}\mathrm{C}$ ($Ba_{1-x}Ca_xF_2$) and 2 h at $T = 950\,^{\circ}\mathrm{C}$ ($Pb_{1-x}Ca_xF_2$). The crystals were grown at a rate of 10 mm per h at $T = 1400\,^{\circ}\mathrm{C}$ ($Ba_{1-x}Ca_xF_2$) and $T = 950\,^{\circ}\mathrm{C}$ ($Pb_{1-x}Ca_xF_2$). After the crucible was transported over the gradient zone the furnace was switched off and the crystals were cooled to room temperature during 8 h for $Ba_{1-x}Ca_xF_2$ and 4 h for $Pb_{1-x}Ca_xF_2$. These rates are faster than the typical crystal growing cooling times of 16–24 h. The resulting samples, which have large single crystal domains, are heavily strained, but optically transparent.

The dopant concentration was measured by powder x-ray diffraction of end chips as well as by Raman scattering along the entire length of each sample. X-ray diffraction measures the average lattice constant, and Raman scattering measures the shift of the T_{2g} symmetry phonon mode. The Raman and x-ray data were converted into mol% CaF_2 concentration, linearly extrapolated via

TABLE I. Nominal and measured average dopant concentrations $x_{\mathrm{Nom.}}$ and x, in mol% for individual mixed crystals; and the dielectric constant ϵ_0 for each host.

$\epsilon_0 = 6.94$	$x_{\mathrm{Nom.}}$	x	$\epsilon_0 = 26.3$	$x_{\mathrm{Nom.}}$	x
BaCa1	2	2.2 ± 0.5	PbCa1	2	2.5 ± 0.3
BaCa2	4	3.1 ± 1.1	PbCa2	10	3.9 ± 0.9
BaCa3	6	5.4 ± 1.1	PbCa3	6	4.0 ± 1.0
BaCa4	8	5.4 ± 1.2	PbCa4	4	4.2 ± 0.2
			PbCa5	8	5.9 ± 1.6

Vegard's law [11], and were found to be in good quantitative agreement. The concentrations were measured at 8–10 places along the side of the samples via Raman scattering and the average values are given in Table I. The $Ba_{1-x}Ca_xF_2$ samples showed significant variation over the sample length for greater than 2% CaF_2, consistent with the onset of the miscibility gap [12]; while the $Pb_{1-x}Ca_xF_2$ samples were inhomogeneous above about 4% CaF_2, again consistent with the phase diagram showing segregation starting at 4–6 mol% CaF_2 [13]. Laue backscattering measurements indicated that the samples are composed of few-mm single crystal domains with slight reorientations between neighboring crystals.

Typical low temperature (1.5 K) THz absorption spectra over a decade in frequency are plotted in Fig. 1 for some of these mixed crystal samples. These spectra show that no sharp impurity-induced absorption lines appear from 2–25 cm^{-1}, including the $Ba_{0.996}Ca_{0.004}F_2$ sample. Such sharp features are typical in the low concentration spectra of aliovalent mixed crystals [9,14].

When TLS make a significant contribution to the absorption, then increasing the sample temperature produces the characteristic bleaching observed in glasses [15]. The predicted temperature-induced change in the absorption coefficient α, is [9]

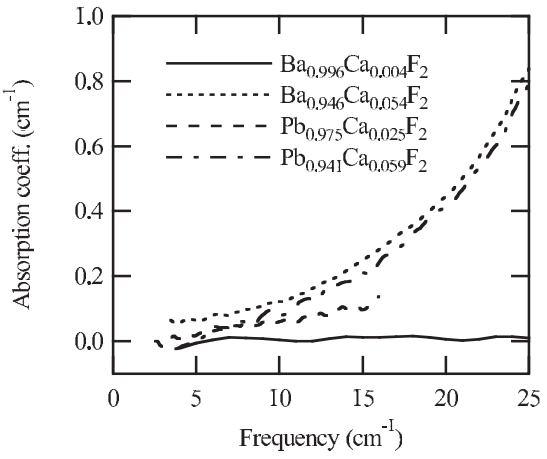

FIG. 1. THz absorption coefficient of different mixed crystals versus frequency at 4.2 K. No sharp defect-induced absorption peaks are observed.

$$\Delta\alpha(T_R, T) = -\frac{4\pi^2}{3c\sqrt{\epsilon_0}}\left(\frac{\epsilon_0 + 2}{3}\right)^2 \omega \bar{P}(\omega)\mu_b^2(\omega)\Delta p(T_R, T), \quad (1)$$

where $\Delta p(T_R, T) \equiv [\tanh(\hbar\omega/2kT_R) - \tanh(\hbar\omega/2kT)]$, and $T_R = 1.5$ K is the reference temperature. The quantity $\bar{P}(\omega)\mu_b^2(\omega)$ is the optical TLS density-of-states (ODOS). Its frequency dependence is due to a cutoff in the high frequency tunneling energy and the onset of excited state transitions [9]. Taking the limit $\bar{P}(\omega \to 0)$ yields $\bar{P}(0)$, the constant spectral density of states per unit frequency range, μ_b is the modulus of the electric dipole transition moment, c is the speed of light, the term in parentheses is the local field correction, ϵ_0 is the dielectric constant, and k is Boltzmann's constant.

The temperature dependent spectra between 1.5 and 7 K are used in conjunction with Eq. (1) to extract the ODOS $\bar{P}(\omega)\mu_b^2(\omega)$. This is done by plotting the data at each individual frequency as $\Delta\alpha$ versus Δp, which are functions of temperature. Figure 2 shows these data for BaCa4 and PbCa4 samples. The breakaway of the data (light symbols) from straight lines at larger Δp, i.e., higher temperatures, is associated with the onset of phonon assisted tunneling absorption, Ref. [14]. The slope of a linear fit through zero is used to extract the ODOS.

The resulting $Ba_{1-x}Ca_xF_2$ and $Pb_{1-x}Ca_xF_2$ ODOS spectra are graphed versus frequency in Fig. 3. The two-level

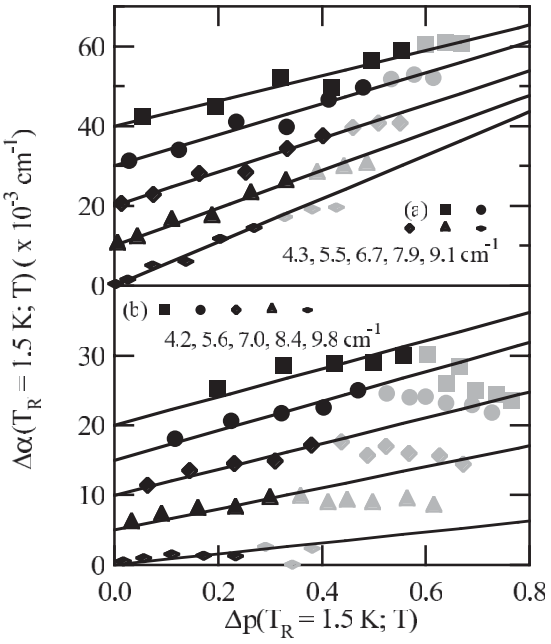

FIG. 2. Fits of $\Delta\alpha$ versus Δp for (a) BaCa4 and (b) PbCa4. The data are offset for clarity and the fitted lines go through zero for each frequency. The temperatures are referenced to $T_R = 1.5$ K, with data points in 1 K increments from 2–10 K for BaCa4; and 3–11, 13, and 15 K for PbCa4. Fitting was done on points up to 7 K (dark symbols) for both samples. Table I gives the dopant concentrations.

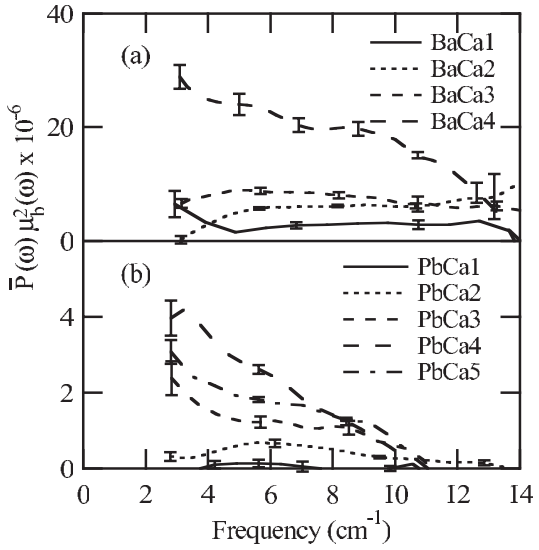

FIG. 3. Measured TLS optical density of states of the mixed crystals versus frequency. The data are obtained from single parameter fits to the temperature dependence of the THz absorption coefficient, and the error bars indicate the standard deviation of the fit. (a) $Ba_{1-x}Ca_xF_2$ and (b) $Pb_{1-x}Ca_xF_2$.

behavior increases monotonically with concentration above a certain minimum value. For the lower concentration BaCa1 and BaCa2 samples, the TLS distribution is not yet completely glasslike since it does not extend below about 4 cm^{-1}. Nonetheless, there is a significant range of two-level behavior and these data are used in Fig. 4. For the BaCa3 and BaCa4 samples, broad distributions of TLS are already present, although saturation has not been reached. The $Pb_{1-x}Ca_xF_2$ data shown in Fig. 3(b) demonstrate negligible ODOS for PbCa1 (2.5%) and a nonmonotonic concentration dependence. For the $Pb_{1-x}Ca_xF_2$ samples, the onset of TLS behavior is very sharp and therefore

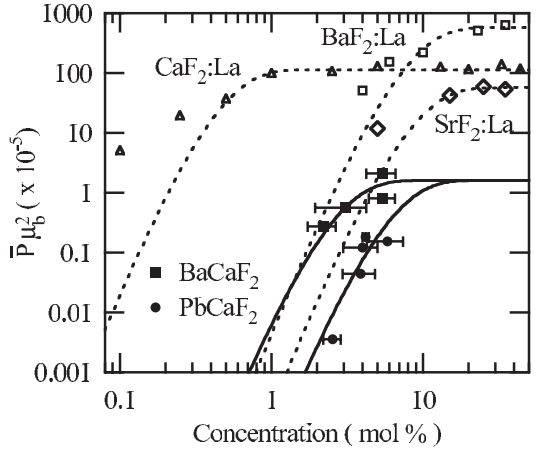

FIG. 4. Critical concentration model fits to the TLS optical density of states for both aliovalent and isovalent mixed crystals. Data points are a weighted average from 3–10 cm^{-1}. The samples are identified in the figure.

sensitive to the precise sample concentrations. The maximum measured ODOS for $Ba_{1-x}Ca_xF_2$ is about one tenth of that in saturated mixed crystals and glasses [9], and the ODOS in $Pb_{1-x}Ca_xF_2$ is about 100th of the saturated values.

Studies with doped alkali halide crystals have already demonstrated that for a given lattice containing a smaller size dopant cation that although single ions may have insufficient volume to tunnel, pairs of such ions can [16]. In both of the systems studied here the dopant ion is the smaller; but there is no evidence of single ion or pair tunneling. We suggest that the TLS effect observed here is associated with a local statistical concentration of dopant ions exceeding a critical value x_c.

Since the probability that a given dopant ion is located in a specific subvolume is (subvolume/crystal volume), the characteristic subvolume for the disordered state needs to be identified. The first step is to introduce a Voronoi tessellation centered on all dopant sites that fills all space [17]. In this way two relevant volumes are defined; V_i is the Voronoi polyhedron volume at site i, and $\bar{V}$ is the expectation value of V_i. The normalized Voronoi volume at site i is then $z_i = V_i/\bar{V}$. Assuming random dopant locations in the crystal and neglecting lattice discreteness, a Poisson Voronoi diagram follows. One feature of the Poisson diagram is that the probability density distribution for z_i can be approximated by the gamma distribution [18]

$$p(z_i) = \frac{z_i^{a-1}}{b^a \Gamma(a)} e^{-z_i/b}, \tag{2}$$

where in three dimensions $a = 5.6333$ and $b = 0.1782$. Summing all Voronoi subvolumes less than a fixed critical value V_c, which is the fitting parameter, and defining $z_c = V_c/\bar{V}$ gives the probability W of locally exceeding a critical concentration

$$W = \int_0^{z_c} dz_i z_i p(z_i). \tag{3}$$

In order to make contact with the ODOS, the saturation level $[\bar{P}\mu_b^2]_{\text{sat}}$ is introduced as a second parameter so that the final expression is

$$\bar{P}\mu_b^2 = [\bar{P}\mu_b^2]_{\text{sat}} \int_0^{z_c} dz_i z_i p(z_i). \tag{4}$$

The critical concentration can be computed from the fit parameter V_c by $x_c = V_{\text{host}}/V_c$, where V_{host} is the volume of the host crystal primitive cell.

This critical concentration model is quite general and may be tested against all the THz data on TLS in mixed crystals. Fits have been carried out for three aliovalent impurity systems, namely CaF_2, BaF_2, and SrF_2 doped with LaF_3 and for the two isovalent systems studied here. The results are shown in Fig. 4 and the parameters given in Table II. The model reproduced well both the delayed increase in TLS absorption with concentration as well as

TABLE II. Critical concentration model fit parameters.

Crystals	$[\bar{P}\mu_b^2]_{\mathrm{sat}}(\times 10^{-5})$	x_c (mol%)
$(CaF_2)_{1-x}(LaF_3)_x$	113 ± 4	0.56 ± 0.06
$(SrF_2)_{1-x}(LaF_3)_x$	56 ± 6	10 ± 2
$(BaF_2)_{1-x}(LaF_3)_x$	570 ± 60	9.5 ± 1.4
$Ba_{1-x}Ca_xF_2$	1.6 ± 0.3	3.2 ± 0.3
$Pb_{1-x}Ca_xF_2$	1.6	7.5 ± 0.05

the saturation at higher concentration. The apparent underestimation by the model at low concentrations for CaF_2:LaF_3 may arise because narrow defect-induced tunneling states appear simultaneously with the incipient broad TLS absorption. In addition, clustering effects would result in higher than random appearance of regions with concentrations exceeding the critical value.

The ODOS for the isovalent systems studied here are obtained by averaging the data between 3 and 10 cm^{-1}, i.e., up to the onset of the excited state transitions. The critical concentration model also shows qualitative agreement with the experimental data. The saturation level obtained by fitting the $Ba_{1-x}Ca_xF_2$ data is 2 orders of magnitude less than for the aliovalent mixed crystals. Most probably this is the result of a smaller dipole moment μ_b since the absorption by TLS created in isovalent systems is not enhanced by charge separation. The large uncertainty in the concentration of $Pb_{1-x}Ca_xF_2$ samples did not permit a reliable determination of $[\bar{P}\mu_b^2]_{\mathrm{sat}}$ so the $Ba_{1-x}Ca_xF_2$ value was applied.

It has been shown that two isovalent mixed crystals, $Ba_{1-x}Ca_xF_2$ and $Pb_{1-x}Ca_xF_2$ do contain significant although not saturated TLS optical density of states. The delayed but rapid onset of TLS behavior with increasing dopant concentration in these minimally disordered monatomic substitutional systems has been successfully modeled with a critical concentration parameter related to the statistics of the dopant distribution in the lattice. The other parameter, the saturation value, indicates that only a small fraction ($\sim 1/1000$) of the critical concentration regions contribute to the collective tunneling phenomenon. This fact suggests a complex energy landscape even for these simple lattice systems.

Finally, the observation of a steplike appearance of TLS with the number density, independent of the local concentration as soon as it exceeds the threshold value, implies that there are no intermediate states—either TLS are present at the saturation level or they are absent. The success of this very simple model for mixed crystals points to a likely connection with the universality of TLS found in glasses.

J. P. W. would like to thank the U.S. Department of Education for financial support. This work was supported by NSF-DMR Grant No. 0301035 and by the Department of Energy Grant No. DE-FG02-04ER46154. P. P. F. acknowledges support from the Russian Foundation of Basic Research (Grant No. 04-03-32836).

[1] R. O. Pohl, X. Liu, and E. Thompson, Rev. Mod. Phys. **74**, 991 (2002).
[2] V. Lubchenko and P. G. Wolynes, Phys. Rev. Lett. **87**, 195901 (2001).
[3] C. Enss, Physica B (Amsterdam) **316**, 12 (2002).
[4] V. G. Karpov, M. I. Klinger, and F. N. Ignat'ev, Solid State Commun. **44**, 333 (1982).
[5] L. Gil, M. A. Ramos, A. Bringer, and U. Buchenau, Phys. Rev. Lett. **70**, 182 (1993).
[6] D. J. Wales, Science **293**, 2067 (2001).
[7] F. J. Walker and A. C. Anderson, Phys. Rev. B **29**, 5881 (1984).
[8] S. A. Kazanskii, JETP Lett. **41**, 224 (1985).
[9] S. A. FitzGerald, A. J. Sievers, and J. A. Campbell, J. Phys. Condens. Matter **13**, 2177 (2001).
[10] D. G. Cahill, S. K. Watson, and R. O. Pohl, Phys. Rev. B **46**, 6131 (1992).
[11] L. Vegard, in *Early Papers on Diffraction of X-rays by Crystals*, edited by J. M. Bijvoet, W. G. Burgers, and G. Hägg (Internatl. Union of Crystallography, Utrecht, 1972), Vol. 2.
[12] P. P. Fedorov, I. I. Buchinskaya, N. A. Ivanovskaya, V. V. Konovalova, S. V. Lavrishchev, and B. P. Sobolev, Dokl. Phys. Chem. (Transl. of Dokl. Akad. Nuak) **401**, 53 (2005).
[13] I. I. Buchinskaya and P. P. Fedorov, Russian J. Inorg. Chem. **43**, 1106 (1998).
[14] S. A. FitzGerald, A. J. Sievers, and J. A. Campbell, J. Phys. Condens. Matter **13**, 2095 (2001).
[15] M. A. Bösch, Phys. Rev. Lett. **40**, 879 (1978).
[16] L. H. Greene and A. J. Sievers, Solid State Commun. **44**, 1235 (1982).
[17] A. Okabe, B. Boots, K. Sugihara, and S. N. Chiu, *Spatial Tessellations: Concepts and Applications of Voronoi Diagrams* (John Wiley & Sons, West Sussex, 1992).
[18] S. Kumar, S. K. Kurtz, J. R. Banavar, and M. G. Sharma, J. Stat. Phys. **67**, 523 (1992).